

LASER INTERFEROMETER GRAVITATIONAL WAVE OBSERVATORY  
- LIGO -  
CALIFORNIA INSTITUTE OF TECHNOLOGY  
MASSACHUSETTS INSTITUTE OF TECHNOLOGY

<b>Document Type</b> <b>LIGO-T970191-03 - D</b> 2/10/98
<b>Test Mass Transmissibility</b>
D. Coyne

*Distribution of this draft:*

Detector

This is an internal working note  
of the LIGO Project.

**California Institute of Technology**  
**LIGO Project - MS 51-33**  
**Pasadena CA 91125**  
Phone (818) 395-2129  
Fax (818) 304-9834  
E-mail: info@ligo.caltech.edu

**Massachusetts Institute of Technology**  
**LIGO Project - MS 20B-145**  
**Cambridge, MA 01239**  
Phone (617) 253-4824  
Fax (617) 253-7014  
E-mail: info@ligo.mit.edu

WWW: <http://www.ligo.caltech.edu/>

## Abstract

Although the internal resonances of the test mass are beyond the Length Sensing and Control (LSC) control bandwidth, any (unintended) magnetic coil drive currents at the test mass resonances will be amplified by the high Q of the test mass. The transmissibility of applied force at the magnet positions to displacement response of the front surface of the LIGO test mass is calculated via finite element analysis. Based upon the transmissibility, the gain attenuation required in the length control system, in order to prevent driving the test mass motion at resonance beyond acceptable limits, may be established.

*Keywords:* test mass, LSC

Revision 01: Added the first symmetric (drum head) frequency by analysis for the Pathfinder optic for comparison with measurement.

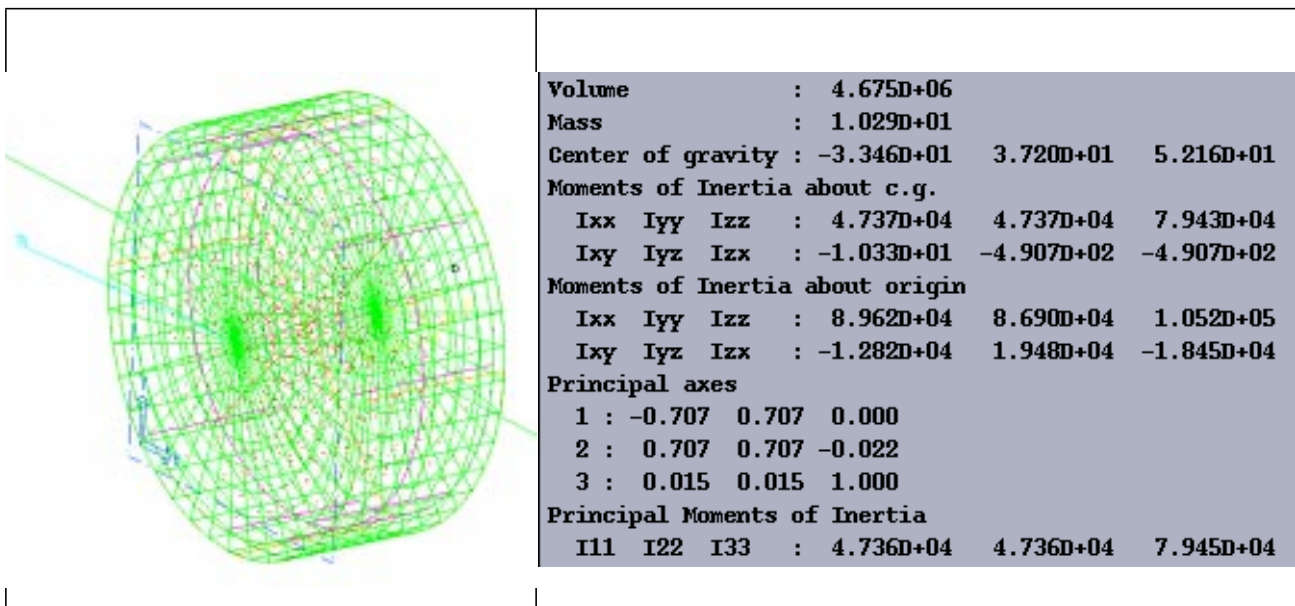
Revision 02: Added section 4 on the integral overlap of the modes with a Gaussian beam (plus a few minor corrections).

Revision 03: Changed the Gaussian beam parameter  $w$  from 35 mm to 45.6 mm, as appropriate for the End Test Mass (ETM) and extended the calculations to cover the first 10 elastic modes.

## 1 END TEST MASS FINITE ELEMENT MODEL

The end test mass (ETM) finite element model is indicated in Figure 1. The optic is a 250 mm diameter, 100 mm thick (at it's maximum) fused silica cylinder with one face wedged at a 2 degree angle. The model is composed of 2160 linear solid brick elements and has the mass properties shown in Figure 1.

Figure (1) Finite Element Model and Mass Properties (units are mm and kg)



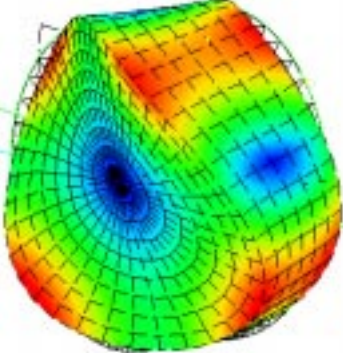
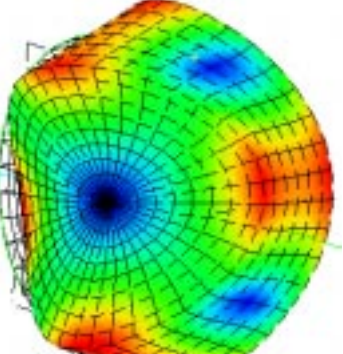
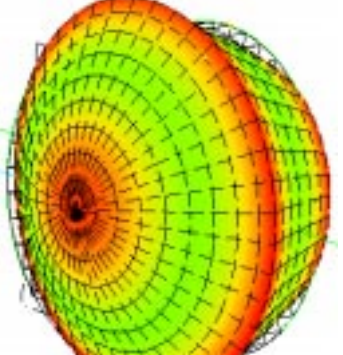
The four magnet positions are at a radial distance of 114.3 mm and at 45, 135, 225 and 315 degrees from the +X (horizontal) axis. The dynamic model does not include the beveled edge of

the optic, nor does it include the four dumbbell magnet standoff and magnet assemblies.

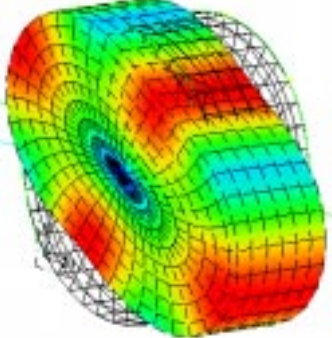
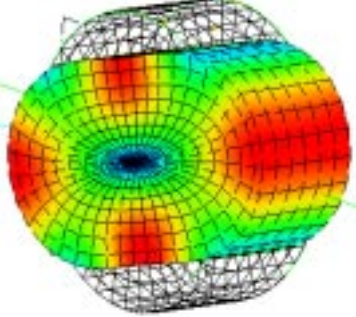
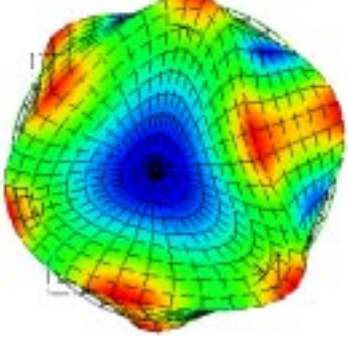
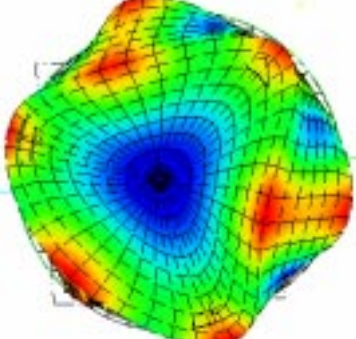
## **2 NATURAL MODES**

The natural modes shapes, frequencies, modal mass and modal stiffness are indicated in Table 1. The analysis indicates a non-axisymmetric pair of modes with astigmatic shape at 6.6 kHz and the first symmetric (drum head) mode at 9.2 kHz.

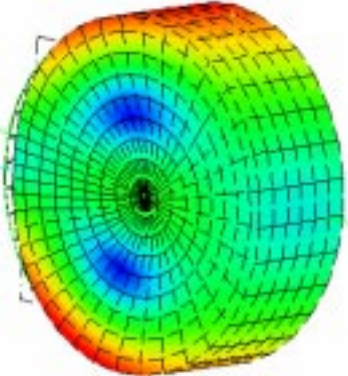
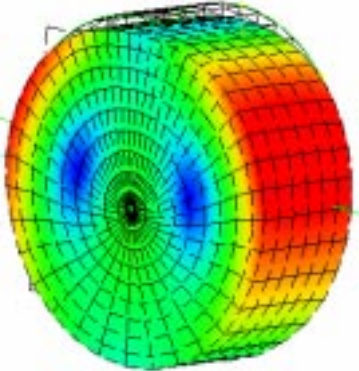
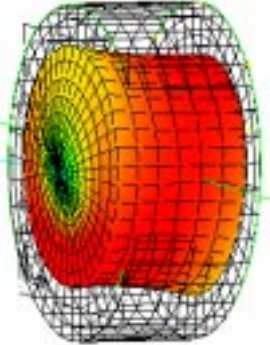
**Table 1. ETM Calculated Modes**

#	<i>Mode Shape</i>	<i>Frequency (Hz)</i>	<i>Modal Mass (<math>10^6</math> gm)</i>	<i>Modal Stiffness (<math>10^{16}</math> N/m)</i>
7		6595	2.53	0.44
8		6595	2.52	0.43
9		9206	3.43	1.15

**Table 1. ETM Calculated Modes**

#	<i>Mode Shape</i>	<i>Frequency (Hz)</i>	<i>Modal Mass (<math>10^6</math> gm)</i>	<i>Modal Stiffness (<math>10^{16}</math> N/m)</i>
10		11217	5.15	2.56
11		11217	5.95	2.95
12		12056	2.20	1.26
13		12057	2.20	1.26

**Table 1. ETM Calculated Modes**

#	Mode Shape	Frequency (Hz)	Modal Mass ( $10^6$ gm)	Modal Stiffness ( $10^{16}$ N/m)
14		12491	3.13	1.93
15		12493	3.25	2.00
16		14475	6.96	5.76

For comparison, the frequencies and Qs measured<sup>1</sup> on the pathfinder optic are indicated in Table 2. The pathfinder optic has the same dimensions as the LIGO ETM with the exception that the wedge angle is 30'. The first measured mode is a drum-head mode at about 9.48 kHz (vs. 9.35 kHz by analysis).

1. S. Kawamura, J. Hazel, M. Barton, Large Optics Suspension Final Design (Mechanical System), LIGO-T970158-06-D, section 4.4, Table 3, 18 Sep 97.

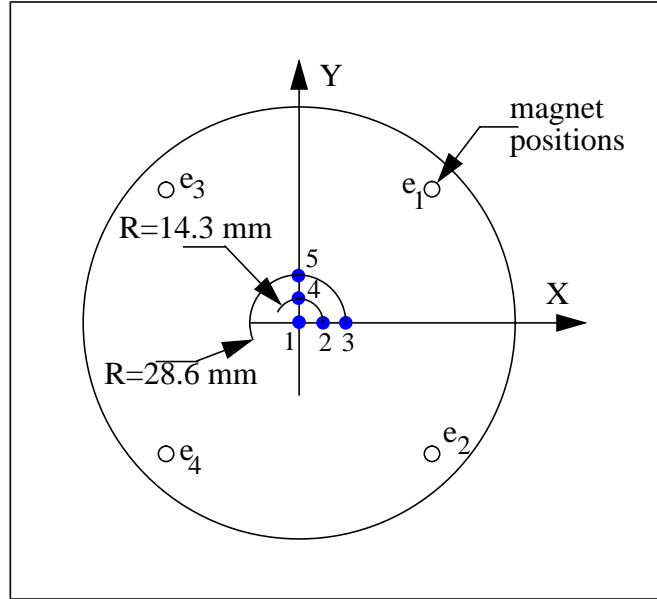
**Table 2: Measured resonance frequencies and Qs of the pathfinder test mass internal modes**  
*(from S. Kawamura, et. al., LIGO-T970158-06-D)*

<i>Mode</i>	<i>Resonance Frequency</i>	<i>Q</i>
Internal Mode	9.4764 kHz	$1.3 \times 10^6$
	22.4215 kHz	$4.6 \times 10^5$
	25.6323 kHz	$2.6 \times 10^6$
	29.4842 kHz	$1.1 \times 10^6$
	29.8662 kHz	Immeasurable
	38.7632 kHz	$8.8 \times 10^5$
	42.7583 kHz	$4.8 \times 10^6$
	47.3324 kHz	$5.4 \times 10^6$
Magnet/Standoff Assembly	7.484 kHz	540

### 3 TRANSMISSIBILITY

In the frequency response analysis, the magnet/voice coil force is assumed to act in the direction parallel to the test mass cylindrical axis despite the fact that the magnet's axis is normal to the wedged surface. The transmissibility (ratio of response displacement to driving force) is given for coherently forcing at the four magnet positions (on the backface of the test mass) with response at the five points (on the front face of the test mass) indicated in Figure 2.

Figure (2) Response Points



The resulting transmissibility functions are indicated in Figure 3. Note that for the 9<sup>th</sup> mode shape (the 3<sup>rd</sup> elastic mode), the variation of the mode shape over the beam waist ( $w_0 \sim 30$  mm) is quite small, as indicated by the modal coefficients for the response points in Figure 2:

$$\begin{aligned} \phi_{9,1} &= 922 & \phi_{9,4} &= 878 \\ \phi_{9,2} &= 878 & \phi_{9,5} &= 778 \\ \phi_{9,3} &= 777 & & \end{aligned}$$

There is approximately a variation of only 5% across the waist of the beam. As a consequence it is not necessary to take the convolution of the Gaussian beam profile and the mode shape to determine the effect on the length.

As a check on the amplitude of response at resonance, the response can be calculated as follows:

The frequency response can be computed through the summation of modal responses:

$$\{\gamma\} = \sum_{k=1}^n \frac{\{F_k\}}{m_k(\omega_k^2 + 2i\zeta\omega\omega_k - \omega^2)} \quad (1)$$

where,



$m_k$  = modal mass

$\gamma$  = modal displacement

$\zeta$  = effective modal viscous damping ratio

$\omega_k$  = natural frequency

$F_k$  = modal (generalized) force

$\omega$  = frequency

subscript k = k<sup>th</sup> mode

At a resonance frequency,  $\omega_0$ :

$$\{\gamma(\omega_0)\} = \sum_{k=1}^n \frac{\{F_k\}}{m_k(\omega_k^2 + 2i\zeta\omega_0\omega_k - \omega_0^2)} \quad (2)$$

or, approximately,

$$\gamma_0 = \frac{F_0}{2im_0\omega_0^2\zeta} \quad (3)$$

The generalized forces (for unrestrained boundary conditions) are:

$$\{F_k\} = [\varphi]^T \{F_e\} \quad (4)$$

where,

$[\varphi]^T$  = mode displacement matrix (mode shapes)

$\{F_e\}$  = applied forces (excitation)

Similarly, the physical displacement is given by:

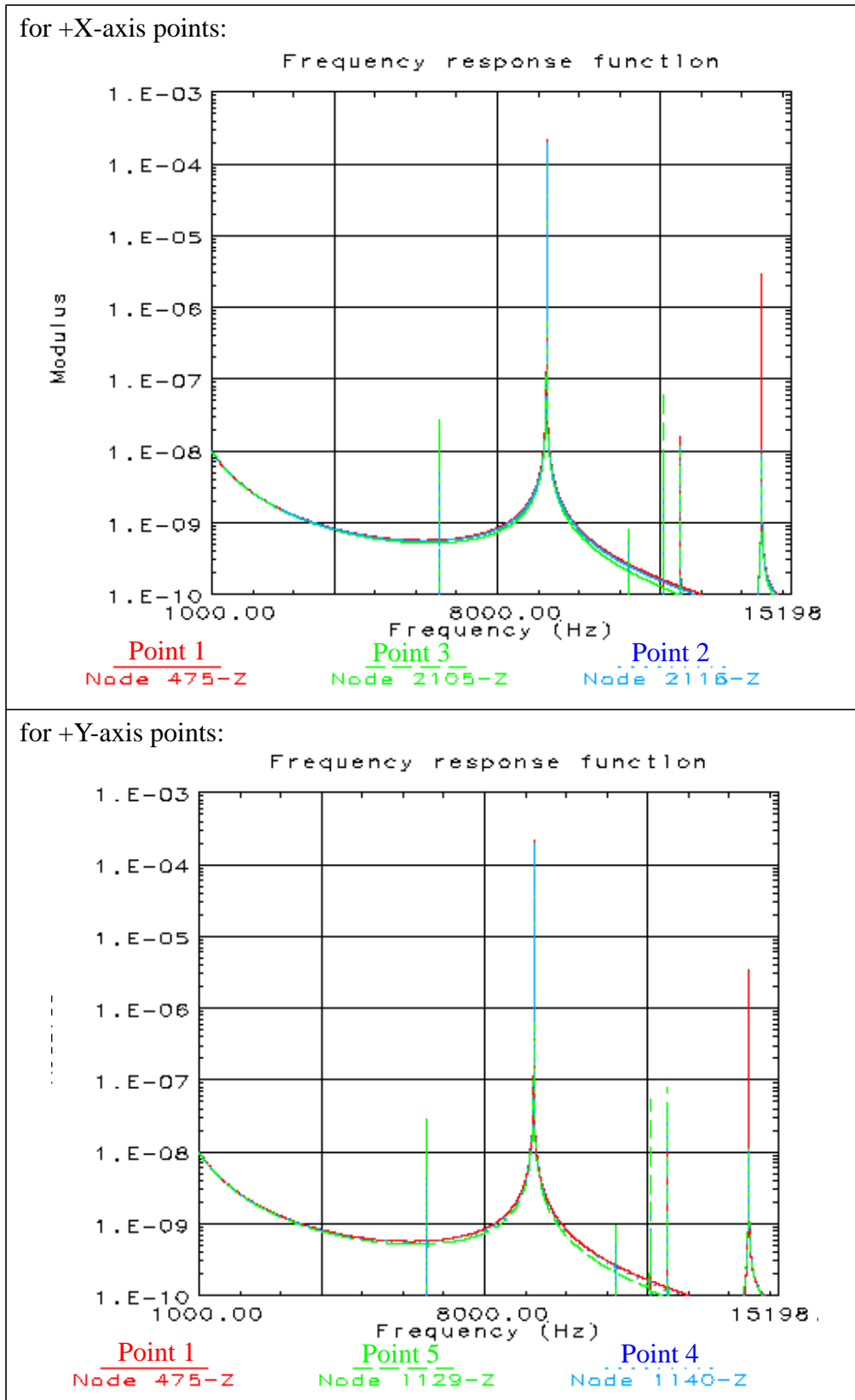
$$\{\delta\} = [\varphi]^T \{\gamma\} \quad (5)$$

or, the displacement at a response point, r, at resonance,  $\omega_0$ , is given as follows:

$$\delta_{r0} = \varphi_{r0}\gamma_0 = \varphi_{r0} \left( \frac{F_0}{2im_0\zeta\omega_0^2} \right) = \varphi_{r0} \left( \frac{\{\varphi_0\}^T \{F_e\}}{2im_0\zeta\omega_0^2} \right) \quad (6)$$

$$|\delta_{r0}| = \varphi_{r0} \left( \frac{\{\varphi_0\}^T \{F_e\}}{2m_0\zeta\omega_0^2} \right) \quad (7)$$

Figure (3) Transmissibility (The "points" are as designated in Figure 2)



If we denote the modal coefficients at each of the 4 magnet positions at the resonance,  $\omega_0$ , as  $\{\varphi_{0e1}, \varphi_{0e2}, \varphi_{0e3}, \varphi_{0e4}\}$  then the transmissibility at a response position,  $\delta_r$ , for a unit force (at each of the 4 magnet positions) is as follows:

$$T_{\delta_r,0} = \frac{\varphi_{r0}(\varphi_{0e1} + \varphi_{0e2} + \varphi_{0e3} + \varphi_{0e4})}{2m_0\zeta\omega_0^2} \quad (8)$$

For  $r$  = center of the front face of the mirror and the first drum head mode ( $\omega_0 = \omega_9 = 9.2$  kHz):

$$\varphi_{0e1} = -510.86$$

$$\varphi_{0e2} = -540.00$$

$$\varphi_{0e3} = -510.86^1$$

$$\varphi_{0e4} = -540.01$$

$$\varphi_{0r} = -922.69$$

$$m_0 = 3.43 \times 10^6$$

$$\zeta = \frac{1}{2Q} = 3.8 \times 10^{-7}$$

Consequently,

$$T_{\delta_r,0} = 2.2 \times 10^{-4} \text{ m/N}$$

which agrees with the IDEAS frequency response calculation (Figure 3).

---

1. Obviously due to the symmetry about the vertical plane (the wedge is vertical),  
 $\varphi_{0e1} = \varphi_{0e3}$  and  $\varphi_{0e2} = \varphi_{0e4}$ .

## 4 MODE INTEGRAL OVERLAP WITH A GAUSSIAN

The cavity length change due to test mass modal motion is sensed by a Gaussian beam. The sensed length change is a Gaussian intensity weighted average of the surface deflection due to the mode. The Gaussian intensity distribution (normalized over the integral) is:

$$I(\hat{r}) = \left(\frac{2}{\pi w^2}\right) e^{-2\left(\frac{r}{w}\right)^2} \quad (9)$$

where the beam waist,  $w = 45.6$  mm (the beam size at the End Test Mass). The physical displacement at a position is related to the modal displacement as follows (from Equation 5):

$$\delta_{\hat{r}k} = \Phi_{\hat{r}k} \gamma_k = \Phi_{\hat{r}k} (T_{\gamma_k} F_e) = T_{\delta_{\hat{r}k}} F_e \quad (10)$$

where the ‘‘transmissibility’’ from coherent force excitation at the four magnet positions to the  $k^{\text{th}}$  modal amplitude is:

$$T_{\gamma_k} = \frac{(\Phi_{ke_1} + \Phi_{ke_2} + \Phi_{ke_3} + \Phi_{ke_4})}{2m_k \zeta_k \omega_k^2} \quad (11)$$

and the transmissibility from coherent force excitation at the four magnet positions to displacement at position  $r$  due to the  $k^{\text{th}}$  mode is:

$$T_{\delta_{\hat{r}k}} = \Phi_{\hat{r}k} T_{\gamma_k} \quad (12)$$

The intensity weighted integral of motion due to the  $k^{\text{th}}$  mode, over surface  $S$ , is given by:

$$\Delta_k = \int_S \delta_{\hat{r}k} I(\hat{r} - \hat{r}_o) dA = T_{\gamma_k} F_e \int_S \Phi_{\hat{r}k} I(\hat{r} - \hat{r}_o) dA \quad (13)$$

where the intensity distribution may be decentered by an alignment tolerance of  $r_o = 1$  mm:

$$\hat{r}_o = (r_o \cos \theta) \hat{i} + (r_o \sin \theta) \hat{j} \quad (14)$$

where  $i$  and  $j$  are unit vectors in the  $x$  and  $y$  coordinate directions.

The  $k^{\text{th}}$  mode integral overlap transmissibility is then:

$$T_{\Delta_k} = \frac{\Delta_k}{F_e} = T_{\gamma_k} \int_S \Phi_{\hat{r}k} I(\hat{r} - \hat{r}_o) dA = T_{\gamma_k} \Gamma_k(\theta) \quad (15)$$

The maximum value of the transmissibility over all values of  $\theta$  is defined as:

$$\max_{\theta}[T_{\Delta_k}] = T_{\gamma_k} \max_{\theta}[\Gamma_k(\theta)] \quad (16)$$

The integrals were performed in Matlab. The IDEAS finite element model (nodal positions, surface node numbers) and mode shapes were imported into Matlab. A two-dimensional spline fit to the non-uniform finite element nodal grid was used to calculate the mode shape on a finer grid within central region of  $\pm 1.925$  beam waists (i.e. the surface S). The results (and the input and some of the intermediate values in the calculation) are given in Tables 3 and 4. The interpolated central regions, S, of the mode shapes are displayed in Table 5.

The Gaussian weighted integral transmissibilities for the first 10 elastic modes are given in the last column of Table 4. The first three pairs of asymmetrical elastic modes, at frequencies of 6.6 kHz, 11.2 kHz and 12.0 kHz, have transmissibilities  $10^6$  times smaller in amplitude than the first symmetric mode, which is  $1.8 \times 10^{-4}$  m/N and occurs at 9.2 kHz. However, one of the fourth pair of asymmetric modes, at 12.5 kHz, has a transmissibility only  $10^4$  times smaller than the first symmetric mode at 9.2 kHz. The second symmetric mode, at 14.4 kHz has a transmissibility only  $10^2$  times smaller than the first symmetric mode.

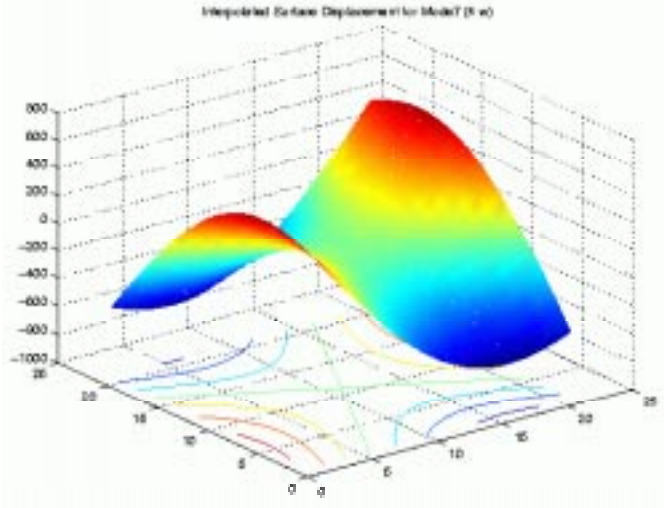
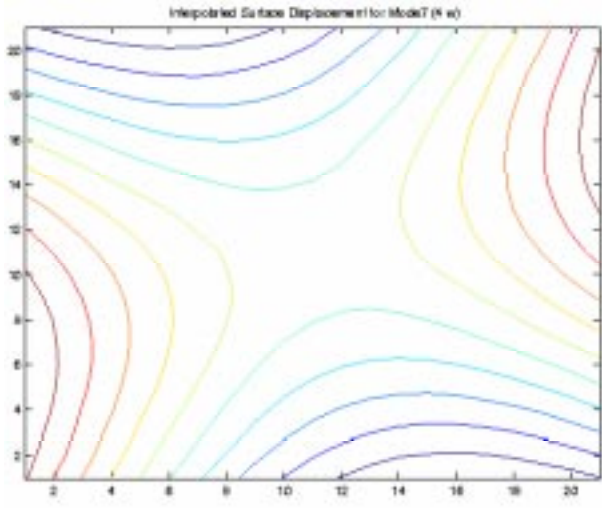
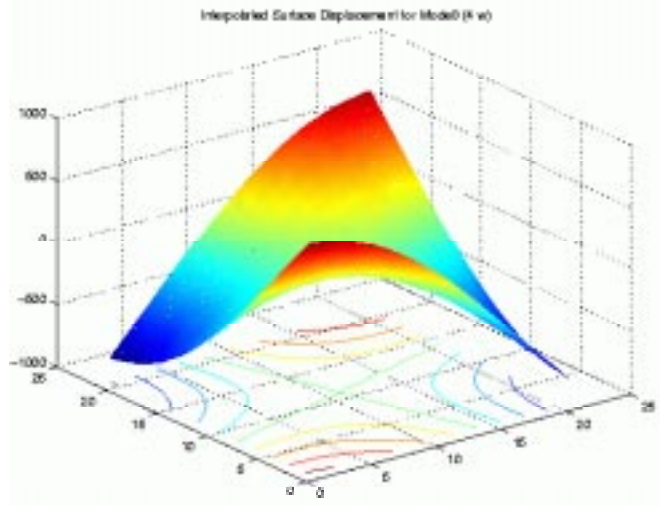
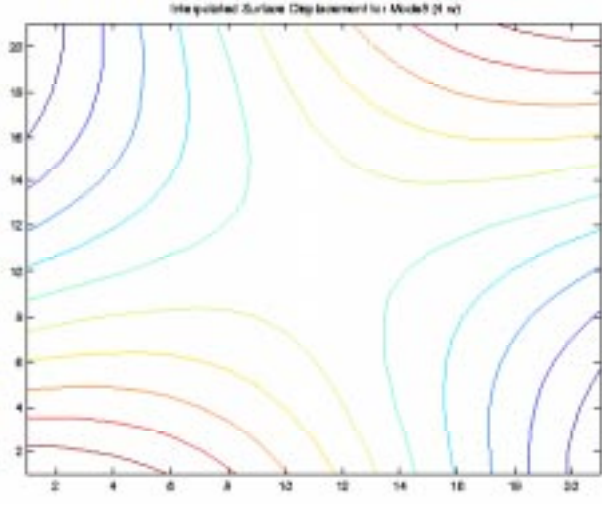
**Table 3. Front Surface Center Transmissibility (modal damping,  $\zeta = 3.8 \times 10^{-7}$ )**

$k$	Frequency (Hz)	Modal Mass ( $10^6$ gm)	Mode Shape Amplitude at Magnet Positions				Modal Transmissibility $T_{\gamma_k}$	Mode Shape Amplitude at the Center $\Phi_{kr}$	Center Displacement Transmissibility $T_{\delta_{\gamma k}}$ (m/N)
			$\Phi_{ke_1}$	$\Phi_{ke_2}$	$\Phi_{ke_3}$	$\Phi_{ke_4}$			
7	6594.849	2.53	-698.538	733.692	694.294	-728.266	3.58e-10	-0.120560	-4.32e-11
8	6594.890	2.52	436.254	-457.122	-442.902	465.661	5.75e-10	-0.187854	-1.08e-10
9	9205.874	3.43	-510.861	-540.005	-510.860	-540.009	-2.41e-07	922.687	-2.22e-04
10	11217.100	5.15	39.646	-26.367	-22.611	8.219	-5.72e-11	-0.336951	1.93e-11
11	11217.130	5.95	-5.828	-4.295	35.452	27.278	-8.67e-11	-0.587398	5.09e-11
12	12056.430	2.20	801.994	17.076	-32.624	-827.427	-4.27e-09	-0.016855	7.20e-11
13	12056.620	2.20	-15.208	829.345	-802.873	32.452	4.56e-09	0.015887	7.24e-11
14	12490.970	3.13	-69.990	-84.481	68.818	5.467	-1.27e-11	0.059799	-7.59e-13
15	12492.620	3.25	-84.598	72.020	-85.613	70.793	-1.80e-09	8.661750	-1.56e-08
16	14474.630	6.96	-115.193	-92.859	-115.195	-92.858	-9.51e-09	305.1300	-2.90e-06

**Table 4. Gaussian Weighted Integral Transmissibility**

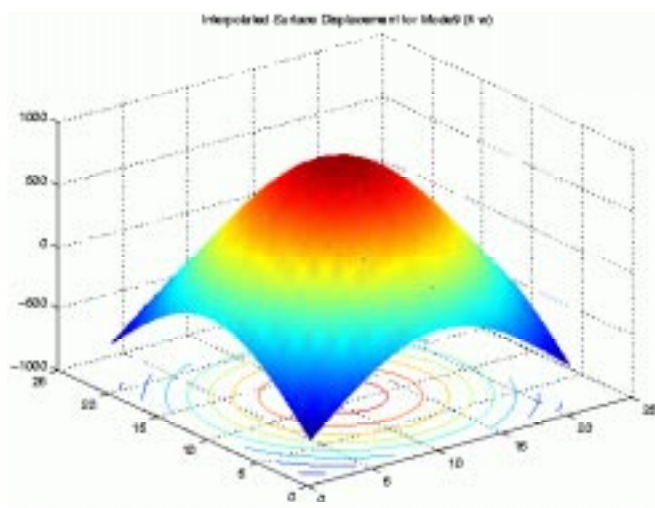
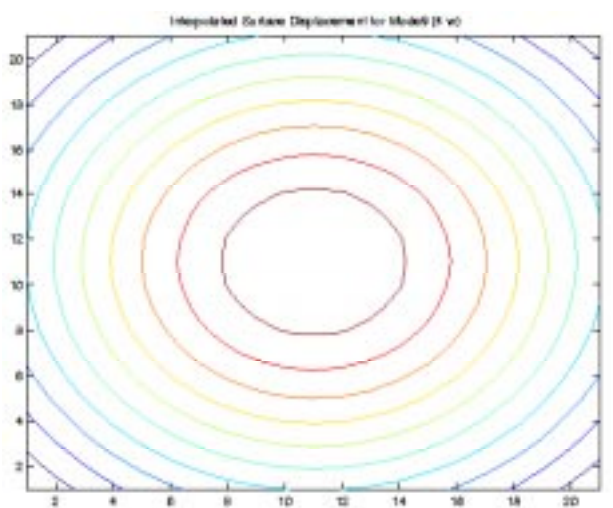
$k$	Frequency (Hz)	Value of the Integral with no Gaussian Intensity Distribution offset $\Gamma_k(r_o \rightarrow 0)$	Maximum Value of the Integral vs. $\theta$ $\max_{\theta}[\Gamma_k(\theta)]$	Gaussian Weighted Integral Transmissibility $\max_{\theta}[T_{\Delta_k}]$ (m/N)
7	6594.849	-0.091977	0.320534	1.15e-10
8	6594.890	-0.172029	0.366452	2.11e-10
9	9205.874	743.9369	743.8522	-1.79e-04
10	11217.100	-0.305398	0.645480	-3.69e-11
11	11217.130	-0.531788	0.895485	-7.77e-11
12	12056.430	-0.016235	0.024689	-1.05e-10
13	12056.620	0.025927	0.039541	1.80e-10
14	12490.970	0.049713	1.214570	-1.54e-11
15	12492.620	7.065459	8.259432	-1.49e-08
16	14474.630	285.8718	287.9970	-2.74e-06

**Table 5. Interpolated Mode Shapes for Z-displacement of the Front Surface Central Region ( $r < 1.92w$ )**

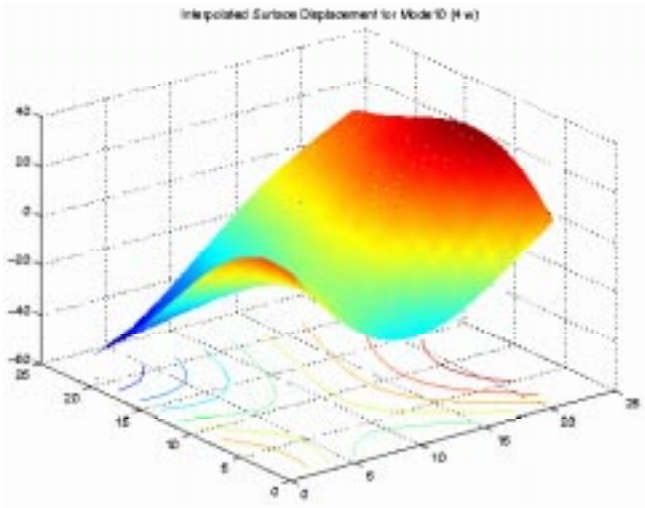
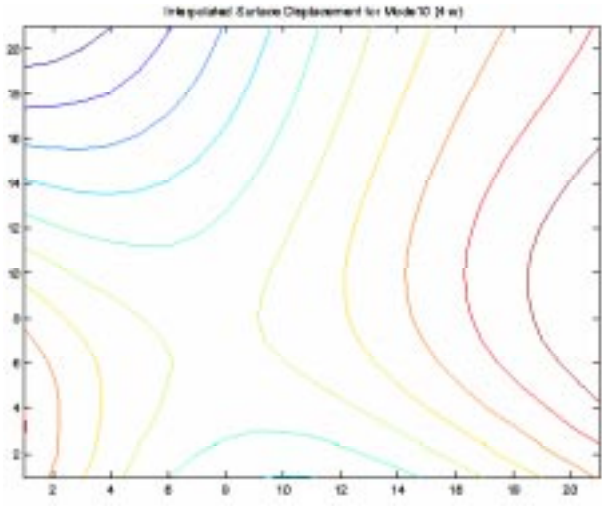
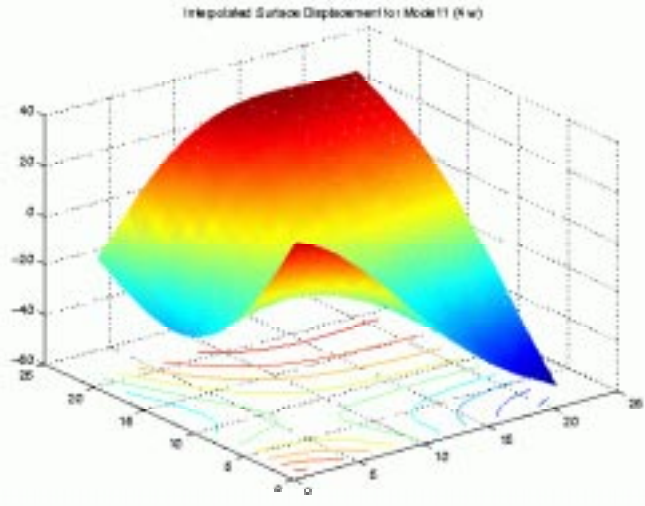
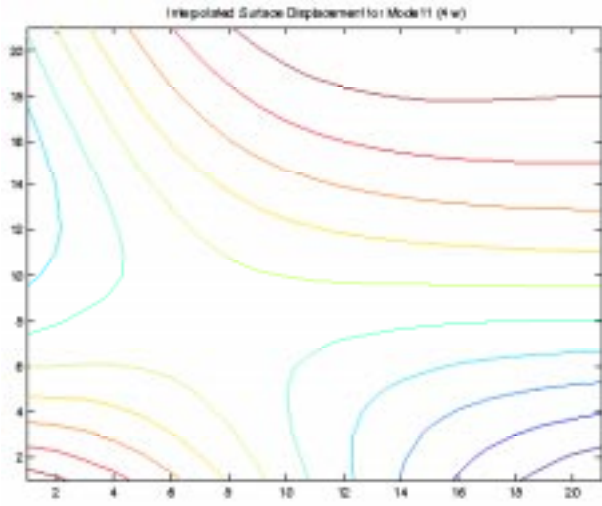
$k$	Frequency (Hz)	Surface Plot	Contour Plot
7	6595		
8	6595		



**Table 5. Interpolated Mode Shapes for Z-displacement of the Front Surface Central Region ( $r < 1.92w$ )**

$k$	Frequency (Hz)	Surface Plot	Contour Plot
9	9206	 <p>Interpolated Surface Displacement for Mode9 (k=9)</p>	 <p>Interpolated Surface Displacement for Mode9 (k=9)</p>

**Table 5. Interpolated Mode Shapes for Z-displacement of the Front Surface Central Region ( $r < 1.92w$ )**

$k$	Frequency (Hz)	Surface Plot	Contour Plot
10	11217		
11	11217		

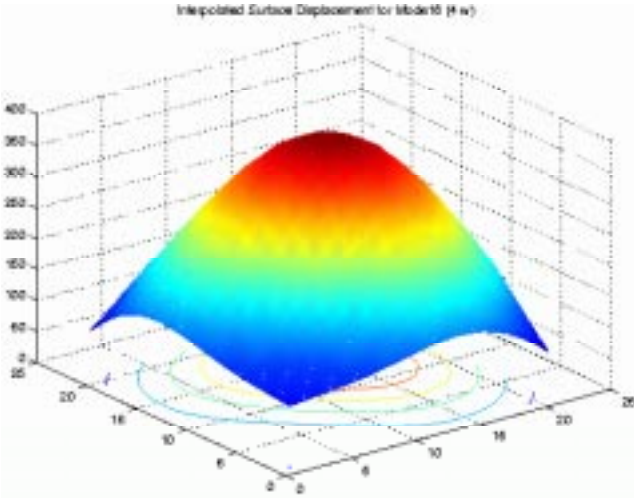
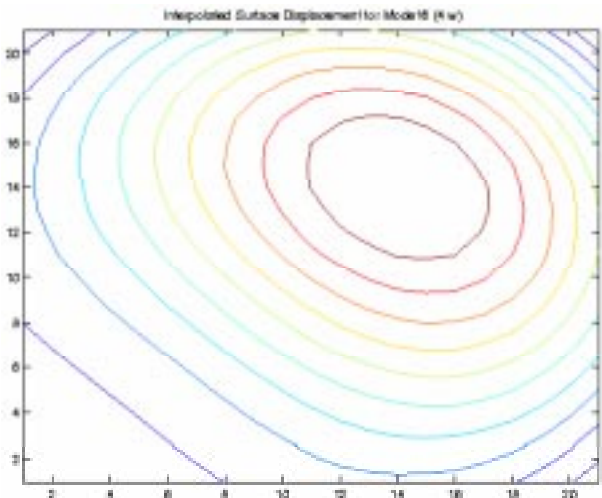
**Table 5. Interpolated Mode Shapes for Z-displacement of the Front Surface Central Region ( $r < 1.92w$ )**

$k$	Frequency (Hz)	Surface Plot	Contour Plot
12	12056.430		
13	12056.620		

**Table 5. Interpolated Mode Shapes for Z-displacement of the Front Surface Central Region ( $r < 1.92w$ )**

$k$	Frequency (Hz)	Surface Plot	Contour Plot
14	12490.970	<p>Interpolated Surface Displacement for Mode 14 (Hz)</p>	<p>Interpolated Surface Displacement for Mode 14 (Hz)</p>
15	12492.620	<p>Interpolated Surface Displacement for Mode 15 (Hz)</p>	<p>Interpolated Surface Displacement for Mode 15 (Hz)</p>

**Table 5. Interpolated Mode Shapes for Z-displacement of the Front Surface Central Region ( $r < 1.92w$ )**

$k$	Frequency (Hz)	Surface Plot	Contour Plot
16	14474.630	 <p>Interpolated Surface Displacement for Mode 16 (Hz)</p>	 <p>Interpolated Surface Displacement for Mode 16 (Hz)</p>